JCTC Journal of Chemical Theory and Computation

Article

pubs.acs.org/JCTC

A Generalized Surface Hopping Algorithm To Model Nonadiabatic Dynamics near Metal Surfaces: The Case of Multiple Electronic Orbitals

Wenjie Dou and Joseph E. Subotnik*

Department of Chemistry, University of Pennsylvania, Philadelphia, Pennsylvania 19104, United States

ABSTRACT: For a molecule with multiple electronic orbitals and many nuclear degrees of freedom near a metal surface, there is a natural embedding of the quantum-classical Liouville equation inside a classical master equation (QCLE-CME) to model nonadiabatic dynamics (*J. Chem. Phys.* **2016**, *145*, 054102). In this paper, we propose a variety of surface hopping algorithms for solving such a QCLE-CME. We find that an augmented surface hopping (A-SH) algorithm works well for propagating such nonadiabatic dynamics (near a metal surface). We expect the present algorithm will be very useful for modeling electrochemical problems in the future.

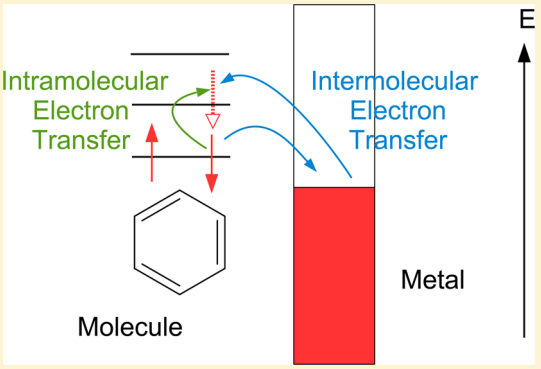

1. INTRODUCTION

Nonadiabatic dynamics near metal surfaces has gained wide interest across the areas of electrochemistry,[1−4] molecular junctions,[5−7] and surface scattering.[8−11] For example, in the area of molecular junctions, coupled electron−nuclear motion has been found to account for a variety of phenomena, including heating or cooling,[12−14] hysteresis,[15−17] instability, or bistability.[18−20] Numerically exact solutions do exist, including numerical renormalization group (NRG) techniques,[21,22] multiconfiguration time dependent Hartree (MC-TDH),[23] quantum Monte Carlo (QMC),[24,25] and the hierarchical quantum master equation (HQME).[26] However, due to the large number of degrees of freedom (DoFs) needed to model a metal, exact methods are limited to relatively small systems. New, inexpensive tools are needed.

To motivate the approach below, on the one hand, consider a molecule (or molecules) that is out of equilibrium in the absence of a metal. For such a problem, many semiclassical methods have been developed to model the nonadiabatic dynamics in the gas phase or solution, including multiple spawning,[27] frozen Gaussian dynamics,[28,29] mean-field dynamics,[30,31] semiclassical initial value dynamics,[32−34] partially linearized density matrix dynamics,[35] generalized quantum master equations,[36,37] and exact factorization dynamics.[38] Tully's fewest switch surface hopping (FSSH)[39] is another important tool for propagating such dynamics and has been successfully applied to many systems, including electron transfer,[40] photochemistry,[41,42] and proton transfer.[30] FSSH was introduced originally by ansatz alone, and recent work has shown a connection between FSSH and the quantum-classical Liouville equation (QCLE).[43−45] Meanwhile, much work has been done over the years to improve decoherence within FSSH.[46−50]

Now on the other hand, consider the simplest molecule possible, a one-level system, near a metal surface. Recently, for such a case, a classical master equation (CME) was derived to model the coupled electron−nuclear motion.[51,52] Just as above, this CME can be solved with a surface hopping (SH) algorithm, that is, classical motion on two different potential energy surfaces (PESs) with stochastic hops between the PESs.[52,53] The main differences between CME-SH and Tully's FSSH are that (1) our CME-SH does not propagate a density matrix and hence we do not have any coherence/decoherence problems, (2) no momentum adjustment has been introduced for CME-SH because there are open electronic boundary conditions, and (3) our CME-SH results recover the correct detailed balance, with the fluctuation−dissipation theorem satisfied exactly, whereas Tully's FSSH recovers detailed balance approximately.[54,55] For completeness, note that ref 56 shows that the CME can be mapped onto a Fokker−Planck equation with explicit forms for the friction and random force, and the resulting friction agrees with the Head-Gordon/Tully result as well as other previously published results.[56−59] In ref 60, we also suggested a simple way to incorporate the effects of level broadening, such that we could extrapolate from the limits of small to large metal−molecule couplings.

Finally, let us return to the case of a realistic molecule on a metal surface. With more than one orbital on the molecule, we can embed the quantum-classical Liouville equation (QCLE) inside a CME (thus forming a QCLE-CME) to account for both intramolecular and metal−molecule interactions. In ref 61, we previously analyzed the natural friction from this QCLE-CME in the adiabatic limit. In this paper, we will now go

Received: January 27, 2017
Published: May 3, 2017

DOI: 10.1021/acs.jctc.7b00094
J. Chem. Theory Comput. 2017, 13, 2430−2439

beyond the adiabatic limit and propose a surface hopping algorithm to approximately solve the full QCLE-CME over a broad range of parameter space that includes the adiabatic and diabatic limits. We will not address broadening in this paper; that topic will be treated in a forthcoming publication. The present surface hopping scheme extends FSSH naturally to the case of a dissipative electronic bath, by connecting FSSH with CME-SH dynamics. As described below, to address decoherence, we will further propose an augmented surface hopping (A-SH) algorithm, which works well across a large range of parameter regimes. We expect this final algorithm (A-SH) will be very useful for modeling realistic systems.

We organize the paper as follows: in section 2, we briefly introduce the QCLE-CME. In section 3, we propose a couple of different surface hopping algorithms to solve the QCLE-CME. We discuss our results in section 4 and conclude in section 5.

1.1. Notation. Below, we will use a "hat", for example, $\hat{O}$, to denote an operator, either for nuclei or for electrons (or both). The subscript "el", for example, $\hat{\rho}_{el}(\mathbf{R},\mathbf{P})$, indicates that the nuclear DoFs are classical (i.e., parameters instead of operators). α and β index nuclear vectors (e.g., R^{α}). Small Roman letters (n, m, k) exclusively index electronic orbitals. Capital Roman letters (I, J, K, L) index electronic states.

2. EQUATION OF MOTION

To be self-consistent, we briefly introduce the QCLE-CME for the coupled electron−nuclear dynamics near metal surfaces. For more details, see ref 61. We divide the total Hamiltonian $\hat{H}$ into three parts: the system $\hat{H}_s$, the bath $\hat{H}_b$, and the system−bath coupling $\hat{H}_c$,

$$\hat{H} = \hat{H}_s + \hat{H}_b + \hat{H}_c \tag{1}$$

$\hat{H}_s$ describes a molecule with electronic orbitals with corresponding creation (annihilation) $\hat{d}_n^+$ ($\hat{d}_m$) operators plus nuclear degrees of freedom (DoFs, with position operator $\hat{R}^{\alpha}$ and momentum operators $\hat{P}^{\alpha}$):

$$\hat{H}_s = \sum_{mn} h_{mn}(\hat{\mathbf{R}})\hat{d}_m^+\hat{d}_n + U(\hat{\mathbf{R}}) + \sum_{\alpha}\frac{\hat{P}_{\alpha}^{\,2}}{2M^{\alpha}} \tag{2}$$

$\hat{H}_b$ describes a metal consisting of a manifold of noninteracting electrons, $\hat{c}_k^+$ ($\hat{c}_k$):

$$\hat{H}_b = \sum_k \epsilon_k \hat{c}_k^+\hat{c}_k \tag{3}$$

The coupling between the system and bath, $\hat{H}_c$, is bilinear

$$\hat{H}_c = \sum_{nk} V_{nk}(\hat{d}_n^+\hat{c}_k + \hat{c}_k^+\hat{d}_n) \tag{4}$$

For the system−bath coupling, we will assume the wide band approximation, that is, the hybridization function $\Gamma_{mn}(\epsilon)$ is independent of ϵ,

$$\Gamma_{mn}(\epsilon) = 2\pi\sum_k V_{mk}V_{nk}\delta(\epsilon-\epsilon_k) = \Gamma_{mn} \tag{5}$$

Following ref 61, assuming weak system−bath coupling, we apply Redfield theory to describe the equation of motion (EOM) for the density matrix of the molecule $\hat{\rho}$,

$$\frac{\partial}{\partial t}\hat{\rho} = -\frac{i}{\hbar}[\hat{H}_s,\hat{\rho}] - \hat{\hat{\mathcal{L}}}_{bs}\hat{\rho} \tag{6}$$

Here, $[\cdot,\cdot]$ is the canonical commutator, and the superoperator $\hat{\hat{\mathcal{L}}}_{bs}$ is

$$\hat{\hat{\mathcal{L}}}_{bs}\hat{\rho} = \frac{1}{\hbar^2}\int_0^{\infty} d\tau\, e^{-i\hat{H}_s t/\hbar}\mathrm{Tr}_b([\hat{H}_{Ic}(t),[\hat{H}_{Ic}(t-\tau), e^{i\hat{H}_s t/\hbar}\hat{\rho}(t)\, e^{-i\hat{H}_s t/\hbar}\otimes\hat{\rho}_b^{eq}]])\, e^{i\hat{H}_s t/\hbar} \tag{7}$$

In the above equation, $\hat{\rho}_b^{eq}$ is the equilibrium density of states for the electronic bath, Tr_b means treating the DoFs in the bath. $\hat{H}_{Ic}(t)$ in eq 7 is written in the interaction picture, $\hat{H}_{Ic}(t) = e^{i(\hat{H}_b+\hat{H}_s)t}\hat{H}_c\, e^{-i(\hat{H}_b+\hat{H}_s)t}$. We refer to eq 6 as a quantum master equation (QME).

We then proceed to perform a partial Wigner transformation for the density operator $\hat{\rho}$ (N_{α} is the total number of nuclear DoFs),

$$\hat{\rho}_{el}(\mathbf{R},\mathbf{P}) \equiv (2\pi\hbar)^{-N_{\alpha}}\int d\mathbf{X}\,\langle\mathbf{R}-\mathbf{X}/2|\hat{\rho}|\mathbf{R}+\mathbf{X}/2\rangle\, e^{i\mathbf{P}\cdot\mathbf{X}/\hbar} \tag{8}$$

In the above equation, $\mathbf{R}$ and $\mathbf{P}$ in $\hat{\rho}_{el}(\mathbf{R},\mathbf{P})$ are now interpreted as position and momentum vectors instead of operators.

After performing a partial Wigner transformation for eq 6 and making the approximation for the classical nuclei (details can be found in ref 61), we arrive at a quantum-classical Liouville equation-classical master equation (QCLE-CME),

$$\frac{\partial}{\partial t}\hat{\rho}_{el}(\mathbf{R},\mathbf{P},t) = \frac{1}{2}\{\hat{H}_s^{el}(\mathbf{R},\mathbf{P}),\hat{\rho}_{el}\} - \frac{1}{2}\{\hat{\rho}_{el},\hat{H}_s^{el}(\mathbf{R},\mathbf{P})\} - \frac{i}{\hbar}[\hat{H}_s^{el},\hat{\rho}_{el}] - \hat{\hat{\mathcal{L}}}_{bs}^{el}(\mathbf{R})\hat{\rho}_{el}(t) \tag{9}$$

Here, $\{\cdot,\cdot\}$ is the Poisson bracket,

$$\{A,B\} = \sum_{\alpha}\left(\frac{\partial A}{\partial R^{\alpha}}\frac{\partial B}{\partial P^{\alpha}} - \frac{\partial A}{\partial P^{\alpha}}\frac{\partial B}{\partial R^{\alpha}}\right) \tag{10}$$

and $\hat{H}_s^{el}$ is the partial Wigner transformation of $\hat{H}_s$

$$\hat{H}_s^{el}(\mathbf{R},\mathbf{P}) = \sum_{mn} h_{mn}(\mathbf{R})\hat{d}_m^+\hat{d}_n + U(\mathbf{R}) + \sum_{\alpha}\frac{P_{\alpha}^{\,2}}{2M^{\alpha}} \equiv \hat{V}(\mathbf{R}) + \sum_{\alpha}\frac{P_{\alpha}^{\,2}}{2M^{\alpha}} \tag{11}$$

The superoperator $\hat{\hat{\mathcal{L}}}_{bs}^{el}(\mathbf{R})$ in eq 9 is now

$$\hat{\hat{\mathcal{L}}}_{bs}^{el}(\mathbf{R})\hat{\rho}_{el}(\mathbf{R},\mathbf{P},t) = \frac{1}{\hbar^2}\int_0^{\infty} d\tau\, e^{-i\hat{H}_s^{el}t/\hbar}tr_b([\hat{H}_{Ic}^{el}(t),[\hat{H}_{Ic}^{el}(t-\tau), e^{i\hat{H}_s^{el}t/\hbar}\hat{\rho}_{el}(t)\, e^{-i\hat{H}_s^{el}t/\hbar}\otimes\hat{\rho}_b^{eq}]])\, e^{i\hat{H}_s^{el}t/\hbar} \tag{12}$$

In the above equation, $\hat{H}_{Ic}^{el}(t) = e^{i(\hat{H}_b+\hat{H}_s^{el})t}\,\hat{H}_c\, e^{-i(\hat{H}_b+\hat{H}_s^{el})t}$. We give a simplified form for the Redfield operator $\hat{\hat{\mathcal{L}}}_{bs}^{el}(\mathbf{R})$ in Appendix A.[62]

Equation 9 reads naturally in a diabatic basis. For surface hopping, however, it is useful to express the QCLE-CME in an adiabatic basis $|\Psi_I^{ad}(\mathbf{R})\rangle$, where

$$\hat{V}(\mathbf{R})|\Psi_I^{ad}(\mathbf{R})\rangle = E_I^{ad}(\mathbf{R})|\Psi_I^{ad}(\mathbf{R})\rangle \tag{13}$$

DOI: 10.1021/acs.jctc.7b00094
J. Chem. Theory Comput. 2017, 13, 2430−2439

In such an adiabatic basis, the QCLE-CME (eq 9) can be written as

$$\frac{\partial}{\partial t}\rho_{IJ}^{\mathrm{ad,el}}(\mathbf{R},\mathbf{P},t) = -\frac{i}{\hbar}(E_I^{\mathrm{ad}}(\mathbf{R}) - E_J^{\mathrm{ad}}(\mathbf{R}))\rho_{IJ}^{\mathrm{ad,el}} - \sum_{\alpha K}\frac{P^\alpha}{M^\alpha}(d_{IK}^\alpha(\mathbf{R})\rho_{KJ}^{\mathrm{ad,el}} - \rho_{IK}^{\mathrm{ad,el}}d_{KJ}^\alpha(\mathbf{R})) - \frac{1}{2}\sum_{\alpha K}\left(F_{IK}^\alpha(\mathbf{R})\frac{\partial\rho_{KJ}^{\mathrm{ad,el}}}{\partial P^\alpha} + \frac{\partial\rho_{IK}^{\mathrm{ad,el}}}{\partial P^\alpha}F_{KJ}^\alpha(\mathbf{R})\right) - \sum_\alpha\frac{P^\alpha}{M^\alpha}\frac{\partial\rho_{IJ}^{\mathrm{ad,el}}}{\partial R^\alpha} - \sum_{KL}\mathcal{L}_{IJ,KL}^{\mathrm{ad,el,bs}}(\mathbf{R})\rho_{KL}^{\mathrm{ad,el}}(t) \tag{14}$$

Here we have defined the force $F_{\mathrm{IJ}}^\alpha \equiv -\langle\Psi_I^{\mathrm{ad}}|\frac{\partial\hat{H}_s^{\mathrm{el}}}{\partial R^\alpha}|\Psi_J^{\mathrm{ad}}\rangle$, and the derivative coupling $d_{IJ}^\alpha \equiv F_{IJ}^\alpha/(E_I^{\mathrm{ad}} - E_J^{\mathrm{ad}})$. In Appendix A, we give an explicit form for the Redfield operator $\hat{\mathcal{L}}_{\mathrm{bs}}^{\mathrm{ad,el}}$ in an adiabatic basis.

Notice that the only difference between the QCLE-CME and the usual QCLE is the Redfield operator ($\hat{\mathcal{L}}_{\mathrm{bs}}^{\mathrm{el}}$) in the latter which exchanges electrons between the molecule and the metal. Because the electron number in the molecule is not conserved, the QCLE-CME must be solved in a many-body (Fock) basis. Below we will use trajectory-based algorithms to solve the QCLE-CME approximately.

3. SURFACE HOPPING ALGORITHMS

Here we propose a surface hopping algorithm to solve the QCLE-CME approximately. This surface hopping algorithm is a natural extension of Tully's FSSH such that we now incorporate the exchange of electrons between molecule and metal. Just as FSSH represents very approximate solutions to the QCLE,[44] this surface hopping algorithm represents a very approximate solution to the QCLE-CME.

Similar to FSSH, for each trajectory, we propagate the density matrix $\hat{\sigma}$ according to

$$\dot{\sigma}_{IJ}^{\mathrm{ad}} = -\sum_{\alpha K}\frac{P^\alpha}{M^\alpha}(d_{IK}^\alpha(\mathbf{R})\sigma_{KJ}^{\mathrm{ad}} - \sigma_{IK}^{\mathrm{ad}}d_{KJ}^\alpha(\mathbf{R})) - \frac{i}{\hbar}(E_I^{\mathrm{ad}}(\mathbf{R}) - E_J^{\mathrm{ad}}(\mathbf{R}))\sigma_{IJ}^{\mathrm{ad}} - \sum_{KL}\mathcal{L}_{IJ,KL}^{\mathrm{ad,el,bs}}(\mathbf{R})\sigma_{KL}^{\mathrm{ad}} \tag{15}$$

as well as position and momentum ($\mathbf{R}$ and $\mathbf{P}$) on the active potential surface (donated as λ),

$$\dot{R}^\alpha = \frac{P^\alpha}{M^\alpha} \tag{16}$$

$$\dot{P}^\alpha = F_{\lambda\lambda}^\alpha \tag{17}$$

Now we have to decide the hopping rates between PES's. In the spirit of Tully's surface hopping, the nuclei hop from population to population. The total change of the population on state J is

$$\dot{\sigma}_{JJ}^{\mathrm{ad}} = -\sum_{\alpha I}\frac{P^\alpha}{M^\alpha}(d_{JI}^\alpha(\mathbf{R})\sigma_{IJ}^{\mathrm{ad}} - \sigma_{JI}^{\mathrm{ad}}d_{IJ}^\alpha(\mathbf{R})) - \sum_{KL}\mathcal{L}_{JJ,KL}^{\mathrm{ad,el,bs}}(\mathbf{R})\sigma_{KL}^{\mathrm{ad}} \tag{18}$$

The first term on the right-hand side (RHS) of the above equation indicates hopping due to derivative coupling, d_{IJ}^α. Following FSSH, we define the hopping rate from I to J to be

$$k_{I\to J}^d = \Theta\left(-2\Re\sum_\alpha\frac{P^\alpha}{M^\alpha}\frac{d_{JI}^\alpha\sigma_{IJ}^{\mathrm{ad}}}{\sigma_{II}^{\mathrm{ad}}}\right) \tag{19}$$

Here the Θ function is defined as

$$\Theta(x) = \begin{cases} x, & \text{if } x \geq 0 \\ 0, & \text{if } x < 0 \end{cases} \tag{20}$$

The second term on the RHS of eq 18 gives an extra hopping due to molecule−metal interaction. This term can be divided into diagonal and off-diagonal contributions:

$$-\sum_{KL}\mathcal{L}_{JJ,KL}^{\mathrm{ad,el,bs}}\sigma_{KL}^{\mathrm{ad}} = -\sum_I\mathcal{L}_{JJ,II}^{\mathrm{ad,el,bs}}\sigma_{II}^{\mathrm{ad}} - \sum_{K\neq L}\mathcal{L}_{JJ,KL}^{\mathrm{ad,el,bs}}\sigma_{KL}^{\mathrm{ad}} \tag{21}$$

Just as in any master equation, the diagonal contribution implies a hopping rate from population I to J of the form

$$k_{I\to J}^{\mathrm{on}} = -\mathcal{L}_{JJ,II}^{\mathrm{ad,el,bs}} \tag{22}$$

To deal with the off-diagonal contribution in eq 21, we will apply a global flux surface hopping (GFSH) scheme,[63] where we denote

$$b_{JJ} = -\sum_{K\neq L}\mathcal{L}_{JJ,KL}^{\mathrm{ad,el,bs}}\sigma_{KL}^{\mathrm{ad}} \tag{23}$$

such that the hopping rate from I to J is given by

$$k_{I\to J}^{\mathrm{off}} = \begin{cases} \dfrac{-b_{II}b_{JJ}}{\sigma_{II}^{\mathrm{ad}}\sum_K\Theta(b_{KK})}, & \text{if } b_{JJ} > 0 \text{ and } b_{II} < 0 \\ 0, & \text{otherwise} \end{cases} \tag{24}$$

Again, the definition of Θ function is given in eq 20. The need for a GFSH hopping rate might well appear superfluous and unjustified here. To that end, we emphasize that there are many other possible rates for the hopping rate here beyond GFSH. In other words, since $\sum_J b_{JJ} = 0$, the best approach would really be to investigate the functional form of $\mathcal{L}_{JJ,KL}^{\mathrm{ad,el,bs}}$ and pair up all hopping terms so that final sum vanishes. With such a pairing in hand, one could construct more natural hopping rates accordingly. However, constructing such positive and negative pairs is tedious; see, for example, eqs 54−57 in Appendix B, and now imagine we had $N \gg 4$ possible charge states and $M \gg 2$ orbitals! Furthermore, in model problems studied thus far, we find that implementing a more rigorous hopping rate yields nearly identical results as the GFSH rates. Thus, for now, we simply use the GFSH rates to hop between surfaces.

Finally, combining the diagonal and off-diagonal contributions, we find the hopping rate induced by $\hat{\mathcal{L}}_{\mathrm{bs}}^{\mathrm{el}}$ is then

$$k_{I\to J}^{\mathcal{L}} = k_{I\to J}^{\mathrm{on}} + k_{I\to J}^{\mathrm{off}} \tag{25}$$

For convenience, we define the total hopping rate

$$k_{I\to J}^{\mathrm{total}} = k_{I\to J}^{\mathrm{d}} + k_{I\to J}^{\mathcal{L}} \tag{26}$$

In eq 26, we add up hopping rates as induced by the derivate coupling operator (k^{d}) and the Redfield operator ($k^{\mathcal{L}}$). Just as in the CME,[52] when hop occurs due to $k^{\mathcal{L}}$, we postulate that

DOI: 10.1021/acs.jctc.7b00094
J. Chem. Theory Comput. 2017, 13, 2430−2439

there should be no momentum adjustment. However, if hop occurs due to k^{d}, we rescale momenta on the direction of the derivative coupling to conserve energy, just as in FSSH.[44] As such, one has constructed a SH scheme that reduces correctly to both FSSH and CME-SH.

Now we can formalize our protocol explicitly:

1. Prepare the initial $\hat{\sigma}$, $\mathbf{R}$, and $\mathbf{P}$. Choose the active PES (say $\lambda = I$).
2. Evolve $\hat{\sigma}$, $\mathbf{R}$, and $\mathbf{P}$ according to eqs 15−17 for a time interval Δt on the active PES ($\lambda = I$).
3. Calculate the hopping rate $k^{\mathrm{d}}_{I\to K}$ and $k^{\mathcal{L}}_{I\to K}$ for all K, according to eqs 19 and 25 (eq 22 plus eq 24). Generate a random number $\xi \in [0,1]$. We now define $S^J_I = \sum_{K=1}^{J} k^{\mathrm{total}}_{I\to K}$
   - If $\xi > S^N_I \Delta t$ (here N is the total number of PESs), the nuclei remain on surface I.
   - Else if $S^{J-1}_I \Delta t < \xi < (S^{J-1}_I + k^{\mathcal{L}}_{I\to J})\Delta t$, the nuclei hop to surface J ($\lambda = J$), without momentum rescaling.
   - Else if $(S^{J-1}_I + k^{\mathcal{L}}_{I\to J})\Delta t < \xi < S^J_I \Delta t$, the nuclei hops to PES J ($\lambda = J$), with momentum rescaling along the direction of the derivative coupling:

$$\mathbf{P}^{\mathrm{new}} = \mathbf{P} + \kappa \mathbf{d}_{IJ}/|\mathbf{d}_{IJ}| \tag{27}$$

   which satisfies

$$\sum_\alpha \frac{(P^{\alpha,\mathrm{new}})^2}{2M^\alpha} + E^{\mathrm{ad}}_J(\mathbf{R}) = \sum_\alpha \frac{(P^\alpha)^2}{2M^\alpha} + E^{\mathrm{ad}}_I(\mathbf{R}) \tag{28}$$

   Among the two roots satisfying eq 28, the root with smaller $|\kappa|$ is chosen.
4. Repeat step 2 and 3 for the desired number of time steps.

3.1. Secular Surface Hopping (sec-SH). The scheme above can be simplified through a secular approximation. In a sec-SH, the GFSH is turned off, that is, $k^{\mathrm{off}} = 0$ in eq 24. Otherwise, the SH algorithm above is unchanged. To motivate why a secular approximation is appealing, consider the long time dynamics of a master equation. Without any nuclear motion, it is well-known that secular master equations must recover the correct equilibrium long time populations.[64] To understand this unique long-time equilibrium feature of secular master equations, note secular master equations set all coherences to zero (in an adiabatic basis) and thus can be written down in a Lindblad form.[65] By contrast, for a nonsecular master equation, again in the adiabatic basis, the correct equilibrium distribution can be achieved only if the coherence vanishes naturally at long times; in other words, a nonsecular master equation can behave correctly at long times only if decoherence is treated properly. Thus, there is a natural trade-off. On the one hand, the secular approximation can recover the correct equilibrium but gives the wrong short time dynamics. On the other hand, the nonsecular approximation gives the correct short time dynamics, but achieving the correct equilibrium is not guaranteed.

Now, we have shown previously that, for the specific Hamiltonian in eqs 1−4, without any nuclear motion, both the nonsecular and secular approximation recover the correct equilibrium populations.[61] Unfortunately, as will be shown below, this feature disappears when nuclear motion is introduced, and only the secular approximation succeeds for long time populations. In particular, with nuclear motion, we will show that the off-diagonal matrix elements do not always decohere to zero according to nonsecular trajectories, and hence the latter can destroy the long-time equilibrium density matrix.

3.2. Augmented Surface Hopping (A-SH). Because nuclear motion can destroy the long time population of an electronic master equation, below, it will be useful to introduce an augmented surface hopping (A-SH) scheme that interpolates between the usual SH and sec-SH approach. That is, at short times, A-SH should recover SH, while at longer times, A-SH should reduce to sec-SH. To connect these two limits, we will hypothesize that the time scale for turning off GFSH is the decoherence rate, that is, the rate of coherence loss lifetime of electronic states as dictated by nuclear motion. Thus, for A-SH, similar to the A-FSSH algorithm in ref 66, we propagate moments $\delta\hat{\mathbf{R}}$ and $\delta\hat{\mathbf{P}}$,

$$\frac{\partial}{\partial t}\delta R^\alpha_{IJ} = \frac{\delta P^\alpha_{IJ}}{M^\alpha} - \sum_{\alpha K}\frac{P^\alpha}{M^\alpha}(d^\alpha_{IK}(\mathbf{R})\delta R^\alpha_{KJ} - \delta R^\alpha_{IK} d^\alpha_{KJ}(\mathbf{R})) - \frac{i}{\hbar}(E^{\mathrm{ad}}_I(\mathbf{R}) - E^{\mathrm{ad}}_J(\mathbf{R}))\delta R^\alpha_{IJ} \tag{29}$$

$$\frac{\partial}{\partial t}\delta P^\alpha_{IJ} = \frac{1}{2}\sum_K (\delta F^\alpha_{IK}\sigma^{\mathrm{ad}}_{KJ} + \sigma^{\mathrm{ad}}_{IK}\delta F^\alpha_{KJ}) - \frac{i}{\hbar}(E^{\mathrm{ad}}_I(\mathbf{R}) - E^{\mathrm{ad}}_J(\mathbf{R}))\delta P^\alpha_{IJ} - \sum_{\alpha K}\frac{P^\alpha}{M^\alpha}(d^\alpha_{IK}(\mathbf{R})\delta P^\alpha_{KJ} - \delta P^\alpha_{IK} d^\alpha_{KJ}(\mathbf{R})) \tag{30}$$

We have defined $\delta F^\alpha_{KJ} = F^\alpha_{KJ} - F^\alpha_{\lambda,\lambda}\delta_{KJ}$. Then, the final decoherence rate is defined as (just as in ref 44)

$$\frac{1}{\tau^{(K,L)}} = \frac{1}{2}\sum_\alpha (F^\alpha_{K,K} - F^\alpha_{L,L})(\delta R^\alpha_{K,K} - \delta R^\alpha_{L,L}) \tag{31}$$

In A-SH, eq 31 is used to turn off the GFSH hopping contributed from off-diagonal matrix elements of K, L. To be explicit, we define

$$\tilde{b}_{JJ} = -\sum_{K\neq L}\mathcal{L}^{\mathrm{ad,el,bs}}_{JJ,KL}\sigma^{\mathrm{ad}}_{KL}\zeta^{K,L} \tag{32}$$

Here $\zeta^{K,L}$ is either 0 or 1. The hopping rate from off-diagonal matrix elements is

$$\tilde{k}^{\mathrm{off}}_{I\to J} = \begin{cases} \dfrac{-\tilde{b}_{II}\tilde{b}_{JJ}}{\sigma^{\mathrm{ad}}_{II}\sum_K \Theta(\tilde{b}_{KK})}, & \text{if } \tilde{b}_{JJ} > 0 \text{ and } \tilde{b}_{II} < 0 \\ 0, & \text{otherwise} \end{cases} \tag{33}$$

If $\zeta^{K,L} = 1$ for all $K \neq L$, $\hat{k}^{\mathrm{off}}_{I\to J} = k^{\mathrm{off}}_{I\to J}$ (eq 24), such that A-SH recovers SH. If $\zeta^{K,L} = 0$ for all $K \neq L$, $\hat{k}^{\mathrm{off}}_{I\to J} = 0$ and A-SH reduces to the sec-SH.

For convenience, we denote

$$\tilde{k}^{\mathcal{L}}_{I\to J} = k^{\mathrm{on}}_{I\to J} + \tilde{k}^{\mathrm{off}}_{I\to J} \tag{34}$$

$$\tilde{k}^{\mathrm{total}}_{I\to J} = k^{\mathrm{d}}_{I\to J} + \tilde{k}^{\mathcal{L}}_{I\to J} \tag{35}$$

We are now prepared to formalize the A-SH protocol. Note that the interpolation in eqs 31−33 is rather ad hoc for now. Our rational for invoking a A-SH decoherence rate will be partially explained below. Our A-SH algorithm is as follows.

DOI: 10.1021/acs.jctc.7b00094
J. Chem. Theory Comput. 2017, 13, 2430−2439

1. Prepare initial $\hat{\sigma}$, $\mathbf{R}$, and $\mathbf{P}$. Choose the active potential surface (say $\lambda = I$). Set $\delta\hat{\mathbf{R}} = 0$, $\delta\hat{\mathbf{P}} = 0$, $\zeta^{K,L} = 1$ (for all $K \neq L$).
2. Evolve $\hat{\sigma}$, $\mathbf{R}$, and $\mathbf{P}$ according to eqs 15−17 for a time interval Δt on the active potential surface. For any $K \neq L$, if $\zeta^{K,L} = 1$, propagate $\delta\hat{\mathbf{R}}$ and $\delta\hat{\mathbf{P}}$ according to eqs 29 and 30.
3. Calculate the hopping rate $k^{\mathrm{d}}_{I\to K}$ and $\tilde{k}^{\mathcal{L}}_{I\to K}$ according to eqs 19 and 34 (eq 22 plus eq 33). Generate a random number $\xi \in [0,1]$. Define $\tilde{S}^J_I = \sum_{K=1}^{J} \hat{k}^{\mathrm{total}}_{I\to K}$
   - If $\xi > \tilde{S}^N_I \Delta t$ (here N is the total number of PESs), the nuclei remain on surface I.
   - Else if $\tilde{S}^{J-1}_I \Delta t < \xi < (\tilde{S}^{J-1}_I + \tilde{k}^{\mathcal{L}}_{I\to J})\Delta t$, the nuclei hops to surface J, without momentum rescaling. Set $\delta\hat{\mathbf{P}} = 0$.
   - Else if $(\tilde{S}^{J-1}_I + \tilde{k}^{\mathcal{L}}_{I\to J})\Delta t < \xi < \tilde{S}^J_I \Delta t$, the nuclei hops to PES J, with momentum rescaling along the direction of the derivative coupling.

$$\mathbf{P}^{\mathrm{new}} = \mathbf{P} + \kappa \mathbf{d}_{IJ}/|\mathbf{d}_{IJ}| \tag{36}$$

$$\sum_\alpha \frac{(P^{\alpha,\mathrm{new}})^2}{2M^\alpha} + E^{\mathrm{ad}}_J(\mathbf{R}) = \sum_\alpha \frac{(P^\alpha)^2}{2M^\alpha} + E^{\mathrm{ad}}_I(\mathbf{R}) \tag{37}$$

   Among the two roots satisfying eq 37, the root with smaller $|k|$ is chosen. Set $\delta\hat{\mathbf{P}} = 0$, $\delta\hat{\mathbf{R}} = 0$.
4. For all $K \neq L$, if $\zeta^{K,L} = 1$, calculate the decoherence rates $\frac{1}{\tau^{(K,L)}}$ and generate a new random number $\xi \in [0,1]$. If $\frac{\Delta t}{\tau^{(K,L)}} > \xi$, set $\zeta^{K,L} = 0$ and set (for all $J = 1,\ldots,N$)

$$\delta\hat{\mathbf{R}}_{K,J} = \delta\hat{\mathbf{P}}_{K,J} = 0 \tag{38}$$

$$\delta\hat{\mathbf{R}}_{J,K} = \delta\hat{\mathbf{P}}_{J,K} = 0 \tag{39}$$

$$\delta\hat{\mathbf{R}}_{L,J} = \delta\hat{\mathbf{P}}_{L,J} = 0 \tag{40}$$

$$\delta\hat{\mathbf{R}}_{J,L} = \delta\hat{\mathbf{P}}_{J,L} = 0 \tag{41}$$

5. Repeat steps 2 through 5 for the desired number of time steps.

3.3. Electronic Friction−Langevin Dynamics (EF-LD).

In the adiabatic limit, where nuclear motion is slow relative to electron transfer, the QCLE-CME can be mapped onto an electronic friction−Langevin dynamics (EF-LD),[61]

$$M^\alpha \ddot{R}^\alpha = \mathcal{F}^\alpha(\mathbf{R}) - \sum_\beta \gamma^{\alpha\beta}(\mathbf{R})\dot{R}^\beta + \delta\mathcal{F}^\alpha(t) \tag{42}$$

Here the mean force and electronic friction are given by

$$\mathcal{F}^\alpha(\mathbf{R}) = -tr_{\mathrm{e}}\left(\frac{\partial \hat{H}^{\mathrm{el}}_{\mathrm{s}}}{\partial R^\alpha}\hat{\sigma}_{\mathrm{eq}}\right) \tag{43}$$

$$\gamma^{\alpha\beta}(\mathbf{R}) = -tr_{\mathrm{e}}\left(\frac{\partial \hat{H}^{\mathrm{el}}_{\mathrm{s}}}{\partial R^\alpha}\hat{\hat{\mathcal{L}}}^{-1}_{\mathrm{el}}\frac{\partial \hat{\sigma}_{\mathrm{eq}}}{\partial R^\beta}\right) \tag{44}$$

In the above equations, tr_{e} implies a trace over the electronic DoFs in the molecule, and $\hat{\sigma}_{\mathrm{eq}} = \frac{1}{Z} e^{-\hat{H}^{\mathrm{el}}_{\mathrm{s}}/(kT)}$ ($Z = tr_e\, e^{-\hat{H}^{\mathrm{el}}_{\mathrm{s}}/(kT)}$). $\hat{\hat{\mathcal{L}}}^{-1}_{\mathrm{el}}$ is the inverse of $\hat{\hat{\mathcal{L}}}_{\mathrm{el}}$, which is defined as $\hat{\hat{\mathcal{L}}}_{\mathrm{el}}(\cdot) \equiv \hat{\hat{\mathcal{L}}}^{\mathrm{el}}_{\mathrm{bs}}(\cdot) + \frac{i}{\hbar}[\hat{H}^{\mathrm{el}}_{\mathrm{s}}, \cdot]$. $\delta\mathcal{F}^\alpha$ is a random force with a correlation function that is Markovian:

$$\langle \delta\mathcal{F}^\alpha(t)\delta\mathcal{F}^\beta(t')\rangle = 2D^{\alpha\beta}(\mathbf{R})\delta(t-t') \tag{45}$$

where the correlation function is

$$D^{\alpha\beta}(\mathbf{R}) = \frac{1}{2}tr_{\mathrm{e}}\left(\frac{\partial \hat{H}^{\mathrm{el}}_{\mathrm{s}}}{\partial R^\alpha}\hat{\hat{\mathcal{L}}}^{-1}_{\mathrm{el}}\left(\frac{\partial \hat{H}^{\mathrm{el}}_{\mathrm{s}}}{\partial R^\beta}\hat{\sigma}_{\mathrm{eq}} + \hat{\sigma}_{\mathrm{eq}}\frac{\partial \hat{H}^{\mathrm{el}}_{\mathrm{s}}}{\partial R^\beta} - 2tr_{\mathrm{e}}\left(\frac{\partial \hat{H}^{\mathrm{el}}_{\mathrm{s}}}{\partial R^\beta}\hat{\sigma}_{\mathrm{eq}}\right)\hat{\sigma}_{\mathrm{eq}}\right)\right) \tag{46}$$

Note that the friction (plus random force) given in eq 44 (plus eq 46) is not exactly equal to the standard form of electronic friction by von Oppen et al.[58] The difference between our friction here and the results from von Oppen[58] is that we do not take level broadening into account in eq 44, due to our approach based on a perturbative treatment of the system−bath coupling. That being said, we have shown previously[61] that the difference between the QCLE-CME friction (in eq 44) and the friction in ref 58 is small for the case of not very strong system−bath coupling and high temperature, such that the two sets of Langevin dynamics should be very similar. For very large system−bath couplings, one must invoke the von Oppen results,[58] which are accurate to infinite order in the system−bath coupling parameter. See also Appendix D.

4. RESULTS AND DISCUSSION

To test our SH algorithms above, we use a donor−acceptor−metal model. The system Hamiltonian is

$$\hat{H}^{\mathrm{el}}_{\mathrm{s}}(x) = E_{\mathrm{D}}(x)\hat{d}^+_{\mathrm{D}}\hat{d}_{\mathrm{D}} + E_{\mathrm{A}}(x)\hat{d}^+_{\mathrm{A}}\hat{d}_{\mathrm{A}} + W(\hat{d}^+_{\mathrm{D}}\hat{d}_{\mathrm{A}} + \hat{d}^+_{\mathrm{A}}\hat{d}_{\mathrm{D}}) + \frac{1}{2}m\omega^2x^2 + \frac{p^2}{2m} \tag{47}$$

In the donor−acceptor−metal model, we have

$$\Gamma_{\mathrm{AA}} = \Gamma, \quad \Gamma_{\mathrm{DD}} = \Gamma_{\mathrm{DA}} = \Gamma_{\mathrm{AD}} = 0 \tag{48}$$

We will further set $E_{\mathrm{D}}(x) = \mathrm{g}x\sqrt{\frac{2m\omega}{\hbar}} + \epsilon_{\mathrm{D}}$ and $E_{\mathrm{A}}(x) = 0$.

In Appendix B, we express the Redfield operator explicitly in the adiabatic basis for this two-level model. We prepare the nuclei with a Boltzmann distribution on the donor (i.e., the acceptor is empty). We use the scheme in ref 67 to convert between the diabatic and adiabatic states. In Appendix C, we show how to calculate the diabatic population $\langle \hat{d}^+_{\mathrm{D}}\hat{d}_{\mathrm{D}}\rangle$ for SHs and EF-LD. We will compare our results against the QME (see Appendix D).

In Figure 1, we work in the regime where W is relatively larger than Γ. We see good agreement between the QME and all SH algorithms (SH, sec-SH, and A-SH), for both diabatic population and kinetic energy. When W and Γ are both large (which is the adiabatic limit, $W = 0.04$, $\Gamma = 0.01$), EF-LD works well for longer dynamics yet fails to recover the correct initial conditions for diabatic population. This failure arises because, according to EF-LD, we assume local equilibrium for electronic states; the transformation for calculating diabatic populations is

DOI: 10.1021/acs.jctc.7b00094
J. Chem. Theory Comput. 2017, 13, 2430−2439

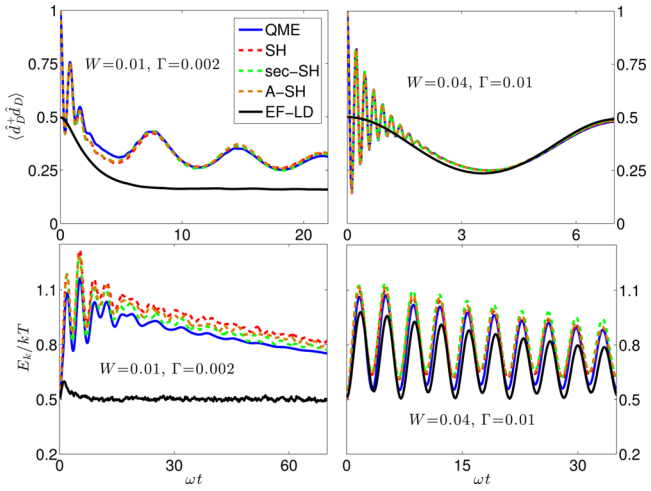

Figure 1. Diabatic electronic population on the donor ($\langle \hat{d}_D^+ \hat{d}_D \rangle$) and the kinetic energy (E_k) as a function of time. The QME results can be considered nearly exact (see Appendix D). All the SH algorithms (SH, sec-SH, A-SH) agree well with the QME. In the adiabatic limit (large W and Γ), EF-LD works for long-time dynamics. kT = 0.01, $\hbar\omega$ = 0.003, g = 0.0075, $\epsilon_D = 2E_r$, and $E_r = g^2/(\hbar\omega)$.

provided in Appendix C. In the nonadiabatic limit (smaller Γ), EF-LD fails completely.

Now we turn to the decoherence issue as implemented in A-SH and to which we alluded in section 3.2. In Figure 2, we

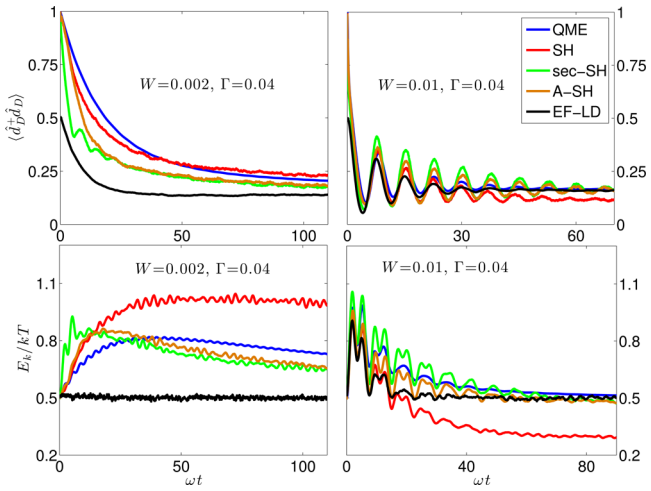

Figure 2. Diabatic electronic population on the donor ($\langle \hat{d}_D^+ \hat{d}_D \rangle$) and the kinetic energy (E_k) as a function of time. SH fails to recover the correct equilibrium. Sec-SH does recover the correct equilibrium but fails for early dynamics. Overall, A-SH performs the best among different SH methods. kT = 0.01, $\hbar\omega$ = 0.003, g = 0.0075, $\epsilon_D = 2E_r$, and $E_r = g^2/(\hbar\omega)$.

plot results for the case that W is relatively small compared with Γ. Now we see differences in the performances of the different SH protocols. Standard SH works well for short time dynamics yet fails to recover the correct equilibrium (either for the diabatic population or the kinetic energy). In fact, the system reaches a different temperature from the bath (as shown by the kinetic energy in Figure 2). Conversely, sec-SH fails at short times but does recover the correct equilibrium at long times. Overall, A-SH agrees best with the QME. Again, EF-LD works best in the adiabatic limit (when W and Γ are both large).

To understand the origin of this behavior (especially for surface hopping), note that in this parameter regime, the GFSH hopping rate (which accounts for the off-diagonal elements of the electronic density matrix $\hat{\sigma}$) is rather large. Now, according to eq 59, if all matrix elements of Γ_{pq} and if all of the Fermi functions do not fluctuate, it follows at long times that, $\sigma_{KL} \to 0$ ($K \neq L$). See the discussion below eq 59. That being said, however, these matrix elements *will* fluctuate because of nuclear motion, and thus, in practice, we may not find that $\sigma_{KL} \to 0$. And thus, the large GFSH rate can destroy long time detailed balance because of an inexact treatment of the coherence in $\hat{\sigma}$.

To address this deficiency, we have hypothesized in this paper that, just as the FSSH algorithm lacks decoherence and cannot properly follow the QCLE without a decoherence correction, so too the FSSH-CME-SH algorithm lacks some decoherence and cannot follow the QCLE-CME. Because this decoherence is necessarily tied to the effect of nuclear motion on electronic dynamics, we therefore propagate nuclear moments (just as in A-FSSH) and turn off GFSH accordingly. Empirically, in Figures 1 and 2, we find that the resulting A-SH algorithm yields very strong results, as A-SH recovers relatively accurate short time dynamics and finds the correct detailed balance at longer times.

That being said, the A-SH algorithm that we introduced in section 3.2 is only a preliminary algorithm, and it is very possible that further improvements can and will be made; in particular, our understanding of decoherence at a metal surface is not yet fully clear or complete (unlike the case in solution). Future work is required to test and improve the A-SH algorithm across many model problems, especially for the case of more than two molecular orbitals in the molecule (where electronic coherence terms can be coupled with each other).

Finally, in the future, it will also be very interesting to test the SH algorithms in an environment where extra phonon friction appears and the correct temperature is maintained: how will A-SH, SH, and sec-SH compare with each other?

5. CONCLUSIONS

We have proposed several efficient algorithms to solve the QCLE-CME, which models the nonadiabatic dynamics for a molecule near a metal surface. These algorithms (i) generalize Tully's FSSH to incorporate the exchange of electrons between molecule and metal and also (ii) generalize the CME-SH to the case of multiple levels in the molecule. Among all the surface hopping algorithms tested here, an augmented surface hopping (A-SH) thus far performs best in most regimes. Further research must strenuously test the algorithms in the condensed phase, especially when extra friction is presented from phonons. The role of decoherence also requires further investigation in the QCLE-CME. Overall, we expect this surface hopping algorithm or variants thereof to be very useful for modeling realistic electrochemical systems and nonadiabatic scattering of molecules off metal surfaces.

APPENDIX A. THE REDFIELD OPERATOR

In the Appendix of ref 61, we have written the Redfield operator in the diabatic basis,

$$\hat{\hat{\mathcal{L}}}^{el}_{bs}\hat{\rho}_{el} = \sum_{mn}\frac{\Gamma_{mn}}{2\hbar}\hat{d}_m^+\hat{S}\mathbb{D}_n\hat{S}^+\hat{\rho}_{el}(t) + \sum_{mn}\frac{\Gamma_{mn}}{2\hbar}\hat{d}_m\hat{S}\mathbb{D}_n^+\hat{S}^+\hat{\rho}_{el}(t) - \sum_{mn}\frac{\Gamma_{mn}}{2\hbar}\hat{d}_m^+\hat{\rho}_{el}(t)\hat{S}\mathbb{D}_n\hat{S}^+ - \sum_{mn}\frac{\Gamma_{mn}}{2\hbar}\hat{d}_m\hat{\rho}_{el}(t)\hat{S}\mathbb{D}_n^+\hat{S}^+ + h.c. \quad (49)$$

DOI: 10.1021/acs.jctc.7b00094
J. Chem. Theory Comput. 2017, 13, 2430−2439

Here $\hat{S}$ is the matrix that diagonalizes the system Hamiltonian $\hat{H}_s^{el}$, with adiabatic PESs E_I^{ad}, $I = 1, ..., N$ (N is total number of PESs). We have defined $(\tilde{\mathbb{D}}_n)_{IJ} \equiv (\hat{S}^+\hat{d}_n\hat{S})_{IJ}(1 - f(E_J^{ad} - E_I^{ad}))$ and $(\mathbb{D}_n)_{IJ} \equiv (\hat{S}^+\hat{d}_n\hat{S})_{IJ}f(E_J^{ad} - E_I^{ad})$. $f(E) = 1/(e^{E/(kT)} + 1)$ is a Fermi function. $\tilde{\mathbb{D}}_n^+/\mathbb{D}_n^+$ is the Hermitian conjugate of $\tilde{\mathbb{D}}_n/\mathbb{D}_n$.

The above equation can be rewritten in an adiabatic basis (noting $\hat{\rho}_{el}^{ad} = \hat{S}^+\hat{\rho}_{el}\hat{S}$),

$$\begin{aligned}\hat{\mathcal{L}}_{bs}^{ad,el}\hat{\rho}_{el}^{ad} &= \sum_{mn}\frac{\Gamma_{mn}}{2\hbar}\hat{S}^+\hat{d}_m^+\hat{S}\tilde{\mathbb{D}}_n\hat{\rho}_{el}^{ad}(t) \\ &+ \sum_{mn}\frac{\Gamma_{mn}}{2\hbar}\hat{S}^+\hat{d}_m\hat{S}\mathbb{D}_n^+\hat{\rho}_{el}^{ad}(t) \\ &- \sum_{mn}\frac{\Gamma_{mn}}{2\hbar}\hat{S}^+\hat{d}_m^+\hat{S}\hat{\rho}_{el}^{ad}(t)\mathbb{D}_n \\ &- \sum_{mn}\frac{\Gamma_{mn}}{2\hbar}\hat{S}^+\hat{d}_m\hat{S}\hat{\rho}_{el}^{ad}(t)\tilde{\mathbb{D}}_n^+ + h.c.\end{aligned} \tag{50}$$

APPENDIX B. THE REDFIELD OPERATOR FOR DONOR–ACCEPTOR METAL MODEL

Now we apply the results above to the two-level model in section 4. We write the diabatic system Hamiltonian in a Fock space,

$$\hat{H}_s^{el} = \begin{pmatrix} 0 & & & \\ & E_D & W & \\ & W & E_A & \\ & & & E_D + E_A \end{pmatrix} + \left(\frac{1}{2}m\omega^2x^2 + \frac{p^2}{2m}\right)\hat{I}_{el} \tag{51}$$

Here $\hat{I}_{el}$ is an (electronic) identity matrix. The annihilation operators $\hat{d}_D$ and $\hat{d}_A$ are

$$\hat{d}_D = \begin{pmatrix} 0 & 1 & 0 & 0 \\ 0 & 0 & 0 & 0 \\ 0 & 0 & 0 & -1 \\ 0 & 0 & 0 & 0 \end{pmatrix}, \quad \hat{d}_A = \begin{pmatrix} 0 & 0 & 1 & 0 \\ 0 & 0 & 0 & 1 \\ 0 & 0 & 0 & 0 \\ 0 & 0 & 0 & 0 \end{pmatrix} \tag{52}$$

The $\hat{S}$ matrix that diagonalizes $\hat{H}_s^{el}$ takes the form

$$\hat{S} = \begin{pmatrix} 1 & & & \\ & \cos\theta & \sin\theta & \\ & -\sin\theta & \cos\theta & \\ & & & 1 \end{pmatrix} \tag{53}$$

For simplicity, below we denote $f(E_I^{ad} - E_J^{ad}) = f_{IJ}$ ($I,J = 1, ..., 4$). We further denote $\Gamma_{aa} = \Gamma \sin^2\theta$, $\Gamma_{bb} = \Gamma \cos^2\theta$, and $\Gamma_{ab} = -\Gamma \cos\theta \sin\theta$. Now we can write the Redfield operator explicitly for the two-level system in the adiabatic basis,

$$\begin{aligned}-(\mathcal{L}_{bs}^{ad,el}\rho_{el}^{ad})_{11} &= -\left(\frac{\Gamma_{aa}}{\hbar}f_{21} + \frac{\Gamma_{bb}}{\hbar}f_{31}\right)\rho_{11}^{ad,el} + \frac{\Gamma_{aa}}{\hbar}f_{12}\rho_{22}^{ad,el} \\ &+ \frac{\Gamma_{bb}}{\hbar}f_{13}\rho_{33}^{ad,el} + \frac{\Gamma_{ab}}{2\hbar}(f_{12} + f_{13})(\rho_{32}^{ad,el} + \rho_{23}^{ad,el})\end{aligned} \tag{54}$$

$$\begin{aligned}-(\mathcal{L}_{bs}^{ad,el}\rho_{el}^{ad})_{22} &= -\left(\frac{\Gamma_{aa}}{\hbar}f_{12} + \frac{\Gamma_{bb}}{\hbar}f_{42}\right)\rho_{22}^{ad,el} + \frac{\Gamma_{aa}}{\hbar}f_{21}\rho_{11}^{ad,el} \\ &+ \frac{\Gamma_{bb}}{\hbar}f_{24}\rho_{44}^{ad,el} - \frac{\Gamma_{ab}}{2\hbar}(f_{13} - f_{43})(\rho_{ad,32}^{el} + \rho_{ad,23}^{el})\end{aligned} \tag{55}$$

$$\begin{aligned}-(\mathcal{L}_{bs}^{ad,el}\rho_{el}^{ad})_{33} &= -\left(\frac{\Gamma_{aa}}{\hbar}f_{43} + \frac{\Gamma_{bb}}{\hbar}f_{13}\right)\rho_{33}^{ad,el} + \frac{\Gamma_{aa}}{\hbar}f_{34}\rho_{44}^{ad,el} \\ &+ \frac{\Gamma_{bb}}{\hbar}f_{31}\rho_{11}^{ad,el} - \frac{\Gamma_{ab}}{2\hbar}(f_{12} - f_{42})(\rho_{32}^{ad,el} + \rho_{23}^{ad,el})\end{aligned} \tag{56}$$

$$\begin{aligned}-(\mathcal{L}_{bs}^{ad,el}\rho_{el}^{ad})_{44} &= -\left(\frac{\Gamma_{aa}}{\hbar}f_{34} + \frac{\Gamma_{bb}}{\hbar}f_{24}\right)\rho_{44}^{ad,el} + \frac{\Gamma_{aa}}{\hbar}f_{43}\rho_{33}^{ad,el} \\ &+ \frac{\Gamma_{bb}}{\hbar}f_{42}\rho_{22}^{ad,el} - \frac{\Gamma_{ab}}{2\hbar}(f_{42} + f_{43})(\rho_{32}^{ad,el} + \rho_{23}^{ad,el})\end{aligned} \tag{57}$$

The coherence term is

$$\begin{aligned}-(\mathcal{L}_{bs}^{ad,el}\rho_{el}^{ad})_{23} &= \chi(\varrho) - \frac{1}{2\hbar}(\Gamma_{aa}f_{12} + \Gamma_{bb}f_{13} + \Gamma_{bb}f_{42} \\ &+ \Gamma_{aa}f_{43})\rho_{23}^{ad,el}\end{aligned} \tag{58}$$

with the complex conjugate $(\mathcal{L}_{bs}^{ad,el}\rho_{el}^{ad})_{32} = (\mathcal{L}_{bs}^{ad,el}\rho_{el}^{ad})_{23}^*$. The second term on the RHS of eq 58 is a natural decoherence term. We have defined $\chi(\varrho)$ in eq 58 as

$$\begin{aligned}\chi(\varrho) = \frac{\Gamma_{ab}}{2\hbar}&((f_{31} + f_{21})\rho_{11}^{ad,el} - (f_{12} - f_{42})\rho_{22}^{ad,el} \\ &- (f_{13} - f_{43})\rho_{33}^{ad,el} - (f_{24} + f_{34})\rho_{44}^{ad,el})\end{aligned} \tag{59}$$

If Γ_{pq} (p,q = a,b) and the Fermi function f_{IJ} do not fluctuate, eqs 54–58 have a simple steady states solution, $\rho_{IJ}^{ad,el} = \frac{1}{Z}\delta_{IJ}\, e^{-E_I^{ad}/(kT)}$ (Z is the normalization factor). We note that, at steady states, $\chi(\varrho) = 0$ and $\rho_{23}^{ad,el} = 0$.

APPENDIX C. DIABATIC POPULATION

In a surface hopping scheme, when calculating the diabatic population, we must transform from the adiabatic basis to a diabatic basis. Following ref 67, the diabatic population $\langle\hat{d}_D^+\hat{d}_D\rangle$ is given

$$\begin{aligned}\langle\hat{d}_D^+\hat{d}_D\rangle = \frac{1}{N_{tra}}\sum_{l=1}^{N_{tra}}&(\cos^2\theta_l\delta_{2,\lambda^l} + \sin^2\theta_l\delta_{3,\lambda^l} \\ &+ 2\sin\theta_l\cos\theta_l\Re(\sigma_{l,23}^{ad,el}) + \delta_{4,\lambda^l})\end{aligned} \tag{60}$$

Here, l is an index for trajectories, N_{tra} is total number of trajectories, and λ is the active potential energy surface. The only difference between eq 60 and eq 11 in ref 67 is that, whereas ref 67 treats a two-state system, formally we are now treating a four-state system in Fock space. Furthermore, note that for state 4, both donor and acceptor are occupied (see the system Hamiltonian, eq 51). As a result, we include the term δ_{4,λ^l} on the right-hand side of eq 60.

In a EF-LD, $\langle\hat{d}_D^+\hat{d}_D\rangle$ is given by averaging local equilibrium population:

$$\langle\hat{d}_D^+\hat{d}_D\rangle = \frac{1}{N_{tra}}\sum_{l=1}^{N_{tra}} tr_e(\hat{\sigma}_{eq}(\mathbf{R}^l)\hat{d}_D^+\hat{d}_D) \tag{61}$$

DOI: 10.1021/acs.jctc.7b00094
J. Chem. Theory Comput. 2017, 13, 2430–2439

APPENDIX D. DETAILS FOR THE QME CALCULATIONS

We write the QME again,

$$\frac{\partial}{\partial t}\hat{\rho} = -\frac{i}{\hbar}[\hat{H}_s, \hat{\rho}] - \hat{\hat{\mathcal{L}}}_{bs}\hat{\rho} \tag{62}$$

For the model we chose in section 4 (eq 47), the corresponding system Hamiltonian with quantum nuclear DoFs is

$$\hat{H}_s = \epsilon_D \hat{d}_D^+ \hat{d}_D + \epsilon_A \hat{d}_A^+ \hat{d}_A + W(\hat{d}_D^+ \hat{d}_A + \hat{d}_A^+ \hat{d}_D) \tag{63}$$

$$+ \hbar\omega\left(\hat{a}^+\hat{a} + \frac{1}{2}\right) + g(\hat{a}^+ + \hat{a})\hat{d}_D^+ \hat{d}_D \tag{64}$$

In the exciton basis, we can express the system Hamiltonian as

$$\hat{H}_s = \begin{bmatrix} \hat{H}_{11} & & & \\ & \hat{H}_{22} & \hat{H}_{23} & \\ & \hat{H}_{32} & \hat{H}_{33} & \\ & & & \hat{H}_{44} \end{bmatrix} \tag{65}$$

where

$$\hat{H}_{11} = \hbar\omega\left(\hat{a}^+\hat{a} + \frac{1}{2}\right) \tag{66}$$

$$\hat{H}_{22} = \hbar\omega\left(\hat{a}^+\hat{a} + \frac{1}{2}\right) + g(\hat{a}^+ + \hat{a}) + \epsilon_D \tag{67}$$

$$\hat{H}_{33} = \hbar\omega\left(\hat{a}^+\hat{a} + \frac{1}{2}\right) + \epsilon_A \tag{68}$$

$$\hat{H}_{44} = \hbar\omega\left(\hat{a}^+\hat{a} + \frac{1}{2}\right) + g(\hat{a}^+ + \hat{a}) + \epsilon_D + \epsilon_A \tag{69}$$

and

$$\hat{H}_{23} = \hat{H}_{32} = W\hat{I}_n \tag{70}$$

$\hat{I}_n$ is the nuclear identity operator. The phonon operator is given by

$$\hat{a}^+\hat{a} = \begin{bmatrix} 0 & & & \\ & 1 & & \\ & & 2 & \\ & & & \ddots \end{bmatrix}, \quad \hat{a} + \hat{a}^+ = \begin{bmatrix} 0 & 1 & & & \\ 1 & 0 & \sqrt{2} & & \\ & \sqrt{2} & 0 & \sqrt{3} & \\ & & \ddots & \ddots & \ddots \end{bmatrix} \tag{71}$$

We will truncate the number of the dimension to N_{ph}. For the parameters we used in the main body of the text, we found good convergences with $N_{ph} = 40$.

The superoperator in eq 62 can be simplified after we diagonalize the system Hamiltonian $\hat{H}_s$.

$$\hat{\hat{\mathcal{L}}}_{bs}\hat{\rho} = \sum_{mn}\frac{\Gamma_{mn}}{2\hbar}\hat{d}_m^+\hat{U}\tilde{\mathbb{I}}_n\hat{U}^+\hat{\rho} + \sum_{mn}\frac{\Gamma_{mn}}{2\hbar}\hat{d}_m\hat{U}\mathbb{I}_n^+\hat{U}^+\hat{\rho} - \sum_{mn}\frac{\Gamma_{mn}}{2\hbar}\hat{d}_m^+\hat{\rho}\hat{U}\mathbb{I}_n\hat{U}^+ - \sum_{mn}\frac{\Gamma_{mn}}{2\hbar}\hat{d}_m\hat{\rho}\hat{U}\tilde{\mathbb{I}}_n^+\hat{U}^+ + h.c. \tag{72}$$

where

$$\hat{d}_D = \begin{bmatrix} 0 & \hat{I}_n & 0 & 0 \\ 0 & 0 & 0 & 0 \\ 0 & 0 & 0 & -\hat{I}_n \\ 0 & 0 & 0 & 0 \end{bmatrix}, \quad \hat{d}_A = \begin{bmatrix} 0 & 0 & \hat{I}_n & 0 \\ 0 & 0 & 0 & \hat{I}_n \\ 0 & 0 & 0 & 0 \\ 0 & 0 & 0 & 0 \end{bmatrix} \tag{73}$$

Here $\hat{U}$ is the matrix that diagonalizes the system Hamiltonian $\hat{H}_s$, with energy levels $\bar{\epsilon}_i$ (i = 1, ..., $4N_{ph}$). We have defined $(\tilde{\mathbb{I}}_n)_{ij} \equiv (\hat{U}^+\hat{d}_n\hat{U})_{ij}(1 - f(\bar{\epsilon}_j - \bar{\epsilon}_i))$ and $(\mathbb{I}_n)_{ij} \equiv (\hat{U}^+\hat{d}_n\hat{U})_{ij}f(\bar{\epsilon}_j - \bar{\epsilon}_i)$.

A few more words are appropriate regarding the validity of the QME. In the regime where the temperature is fairly large, QME dynamics should be relatively reliable, except for broadening effects. For the donor−acceptor−metal model in section 4 (eqs 47 and 48), we see that nuclear motion is coupled only to the donor, whereas any broadening effects on the donor should be relatively small (because the donor is coupled only indirectly to the continuum through the acceptor). Thus, overall, we expect the QME should be quantitively accurate. Furthermore, in the same vein, the electronic friction in eq 44 should also be accurate here, in complete agreement with the von Oppen friction.

AUTHOR INFORMATION

Corresponding Author

*E-mail: subotnik@sas.upenn.edu.

ORCID

Wenjie Dou: 0000-0001-5410-6183

Funding

This material is based upon work supported by the (U.S.) Air Force Office of Scientific Research (USAFOSR) PECASE award under AFOSR Grant No. FA9950-13-1-0157. J.E.S. acknowledges a Camille and Henry Dreyfus Teacher Scholar Award and a David and Lucille Packard Fellowship.

Notes

The authors declare no competing financial interest.

ACKNOWLEDGMENTS

We thank Amber Jain for helpful discussions.

REFERENCES

(1) Nitzan, A. Electron transmission through molecules and molecular interfaces. *Annu. Rev. Phys. Chem.* **2001**, *52*, 681−750.

(2) Bartels, C.; Cooper, R.; Auerbach, D. J.; Wodtke, A. M. Energy transfer at metal surfaces: the need to go beyond the electronic friction picture. *Chem. Sci.* **2011**, *2*, 1647−1655.

(3) Mohr, J.-H.; Schmickler, W. Exactly Solvable Quantum Model for Electrochemical Electron-Transfer Reactions. *Phys. Rev. Lett.* **2000**, *84*, 1051.

(4) Mishra, A. K.; Waldeck, D. H. A Unified Model for the Electrochemical Rate Constant That Incorporates Solvent Dynamics. *J. Phys. Chem. C* **2009**, *113*, 17904.

(5) Galperin, M.; Ratner, M. A.; Nitzan, A.; Troisi, A. Nuclear Coupling and Polarization in Molecular Transport Junctions: Beyond Tunneling to Function. *Science* **2008**, *319*, 1056.

(6) Nitzan, A.; Ratner, M. A. Electron transport in molecular wire junctions. *Science* **2003**, *300*, 1384.

(7) Galperin, M.; Ratner, M. A.; Nitzan, A. Molecular transport junctions: vibrational effects. *J. Phys.: Condens. Matter* **2007**, *19*, 103201.

DOI: 10.1021/acs.jctc.7b00094
J. Chem. Theory Comput. 2017, 13, 2430−2439

(8) Huang, Y.; Rettner, C. T.; Auerbach, D. J.; wodtke, A. M. Vibrational Promotion of Electron Transfer. *Science* **2000**, *290*, 111−114.
(9) Wodtke, A. M.; Tully, J. C.; Auerbach, D. J. Electronically non-adiabatic interactions of molecules at metal surfaces: Can we trust the Born-Oppenheimer approximation for surface chemistry? *Int. Rev. Phys. Chem.* **2004**, *23*, 513.
(10) Shenvi, N.; Roy, S.; Tully, J. C. Dynamical Steering and Electronic Excitation in NO Scattering from a Gold Surface. *Science* **2009**, *326*, 829−832.
(11) Saalfrank, P.; Füchsel, G.; Monturet, S.; Tremblay, J. C.; Klamroth, T. Theory of Non-adiabatic Molecular Dynamics at Surfaces. In *Dynamics of Gas-Surface Interactions: Atomic-level Understanding of Scattering Processes at Surfaces*; Díez Muiño, R., Busnengo, H. F., Eds.; Springer: Berlin Heidelberg, 2013; pp 323−348.
(12) Kaasbjerg, K.; Novotný, T.; Nitzan, A. Charge-carrier-induced frequency renormalization, damping, and heating of vibrational modes in nanoscale junctions. *Phys. Rev. B: Condens. Matter Mater. Phys.* **2013**, *88*, 201405.
(13) Koch, J.; von Oppen, F.; Oreg, Y.; Sela, E. Thermopower of single-molecule devices. *Phys. Rev. B: Condens. Matter Mater. Phys.* **2004**, *70*, 195107.
(14) Arrachea, L.; Bode, N.; von Oppen, F. Vibrational cooling and thermoelectric response of nanoelectromechanical systems. *Phys. Rev. B: Condens. Matter Mater. Phys.* **2014**, *90*, 125450.
(15) Galperin, M.; Ratner, M. A.; Nitzan, A. Hysteresis, Switching, and Negative Differential Resistance in Molecular Junctions: A Polaron Model. *Nano Lett.* **2005**, *5*, 125.
(16) Wu, S. W.; Ogawa, N.; Nazin, G. V.; Ho, W. Conductance Hysteresis and Switching in a Single-Molecule Junction. *J. Phys. Chem. C* **2008**, *112*, 5241.
(17) Lörtscher, E.; Ciszek, J.; Tour, J.; Riel, H. Reversible and controllable switching of a single-molecule junction. *Small* **2006**, *2*, 973.
(18) Siddiqui, L.; Ghosh, A. W.; Datta, S. Phonon runaway in carbon nanotube quantum dots. *Phys. Rev. B: Condens. Matter Mater. Phys.* **2007**, *76*, 085433.
(19) Härtle, R.; Thoss, M. Vibrational instabilities in resonant electron transport through single-molecule junctions. *Phys. Rev. B: Condens. Matter Mater. Phys.* **2011**, *83*, 125419.
(20) Wilner, E.; Wang, H.; Cohen, G.; Thoss, M.; Rabani, E. Bistability in a nonequilibrium quantum system with electron-phonon interactions. *Phys. Rev. B: Condens. Matter Mater. Phys.* **2013**, *88*, 045137.
(21) Bulla, R.; Costi, T. A.; Pruschke, T. Numerical renormalization group method for quantum impurity systems. *Rev. Mod. Phys.* **2008**, *80*, 395−450.
(22) Anders, F. B.; Schiller, A. Real-Time Dynamics in Quantum-Impurity Systems: A Time-Dependent Numerical Renormalization-Group Approach. *Phys. Rev. Lett.* **2005**, *95*, 196801.
(23) Thoss, M.; Kondov, I.; Wang, H. Correlated electron-nuclear dynamics in ultrafast photoinduced electron-transfer reactions at dye-semiconductor interfaces. *Phys. Rev. B: Condens. Matter Mater. Phys.* **2007**, *76*, 153313.
(24) Mühlbacher, L.; Rabani, E. Real-Time Path Integral Approach to Nonequilibrium Many-Body Quantum Systems. *Phys. Rev. Lett.* **2008**, *100*, 176403.
(25) Cohen, G.; Gull, E.; Reichman, D. R.; Millis, A. J. Green's Functions from Real-Time Bold-Line Monte Carlo Calculations: Spectral Properties of the Nonequilibrium Anderson Impurity Model. *Phys. Rev. Lett.* **2014**, *112*, 146802.
(26) Schinabeck, C.; Erpenbeck, A.; Härtle, R.; Thoss, M. Hierarchical quantum master equation approach to electronic-vibrational coupling in nonequilibrium transport through nanosystems. *Phys. Rev. B: Condens. Matter Mater. Phys.* **2016**, *94*, 201407.
(27) Ben-Nun, M.; Martinez, T. J. Nonadiabatic molecular dynamics: Validation of the multiple spawning method for a multidimensional problem. *J. Chem. Phys.* **1998**, *108*, 7244.
(28) Heller, E. Frozen Gaussians: A very simple semiclassical approximation. *J. Chem. Phys.* **1981**, *75*, 2923.
(29) White, A.; Tretiak, S.; Mozyrsky, D. Coupled wave-packets for non-adiabatic molecular dynamics: a generalization of Gaussian wave-packet dynamics to multiple potential energy surfaces. *Chem. Sci.* **2016**, *7*, 4905.
(30) Fang, J.-Y.; Hammes-Schiffer, S. Comparison of surface hopping and mean field approaches for model proton transfer reactions. *J. Chem. Phys.* **1999**, *110*, 11166.
(31) Bellonzi, N.; Jain, A.; Subotnik, J. E. An assessment of mean-field mixed semiclassical approaches: Equilibrium population and algorithm stability. *J. Chem. Phys.* **2016**, *144*, 154110.
(32) Meyer, H.-D.; Miller, W. H. A classical analog for electronic degrees of freedom in nonadiabatic collision processes. *J. Chem. Phys.* **1979**, *70*, 3214.
(33) Sun, X.; Miller, W. H. Semiclassical initial value representation for electronically nonadiabatic molecular dynamics. *J. Chem. Phys.* **1997**, *106*, 6346.
(34) Stock, G.; Thoss, M. Semiclassical Description of Nonadiabatic Quantum Dynamics. *Phys. Rev. Lett.* **1997**, *78*, 578.
(35) Huo, P.; Coker, D. F. Consistent schemes for non-adiabatic dynamics derived from partial linearized density matrix propagation. *J. Chem. Phys.* **2012**, *137*, 22A535.
(36) Shi, Q.; Geva, E. A new approach to calculating the memory kernel of the generalized quantum master equation for an arbitrary system-bath coupling. *J. Chem. Phys.* **2003**, *119*, 12063.
(37) Kelly, A.; Brackbill, N.; Markland, T. E. Accurate nonadiabatic quantum dynamics on the cheap: Making the most of mean field theory with master equations. *J. Chem. Phys.* **2015**, *142*, 094110.
(38) Min, S. K.; Agostini, F.; Gross, E. Coupled-Trajectory Quantum-Classical Approach to Electronic Decoherence in Nonadiabatic Processes. *Phys. Rev. Lett.* **2015**, *115*, 073001.
(39) Tully, J. C. Molecular dynamics with electronic transitions. *J. Chem. Phys.* **1990**, *93*, 1061−1071.
(40) Landry, B. R.; Subotnik, J. E. How to recover Marcus theory with fewest switches surface hopping: Add just a touch of decoherence. *J. Chem. Phys.* **2012**, *137*, 22A513.
(41) Petit, A. S.; Subotnik, J. E. How to calculate linear absorption spectra with lifetime broadening using fewest switches surface hopping trajectories: A simple generalization of ground-state Kubo theory. *J. Chem. Phys.* **2014**, *141*, 014107.
(42) Tempelaar, R.; van der Vegte, C. P.; Knoester, J.; Jansen, T. L. C. Surface hopping modeling of two-dimensional spectra. *J. Chem. Phys.* **2013**, *138*, 164106.
(43) Kapral, R.; Ciccotti, G. Mixed quantum-classical dynamics. *J. Chem. Phys.* **1999**, *110*, 8919.
(44) Subotnik, J. E.; Ouyang, W.; Landry, B. R. Can we derive Tully's surface-hopping algorithm from the semiclassical quantum Liouville equation? Almost, but only with decoherence. *J. Chem. Phys.* **2013**, *139*, 214107.
(45) Kapral, R. Surface hopping from the perspective of quantum-classical Liouville dynamics. *Chem. Phys.* **2016**, *481*, 77−83.
(46) Subotnik, J. E.; Shenvi, N. A new approach to decoherence and momentum rescaling in the surface hopping algorithm. *J. Chem. Phys.* **2011**, *134*, 024105.
(47) Neria, E.; Nitzan, A. Semiclassical evaluation of nonadiabatic rates in condensed phases. *J. Chem. Phys.* **1993**, *99*, 1109.
(48) Prezhdo, O. V.; Rossky, P. J. Mean-field molecular dynamics with surface hopping. *J. Chem. Phys.* **1997**, *107*, 825.
(49) Larsen, R. E.; Bedard-Hearn, M. J.; Schwartz, B. J. Exploring the Role of Decoherence in Condensed-Phase Nonadiabatic Dynamics: A Comparison of Different Mixed Quantum/Classical Simulation Algorithms for the Excited Hydrated Electron. *J. Phys. Chem. B* **2006**, *110*, 20055.
(50) Subotnik, J. E.; Jain, A.; Landry, B.; Petit, A.; Ouyang, W.; Bellonzi, N. Understanding the Surface Hopping View of Electronic Transitions and Decoherence. *Annu. Rev. Phys. Chem.* **2016**, *67*, 387.

DOI: 10.1021/acs.jctc.7b00094
J. Chem. Theory Comput. 2017, 13, 2430−2439

(51) Elste, F.; Weick, G.; Timm, C.; von Oppen, F. Current-induced conformational switching in single-molecule junctions. *Appl. Phys. A: Mater. Sci. Process.* **2008**, *93*, 345−354.
(52) Dou, W.; Nitzan, A.; Subotnik, J. E. Surface hopping with a manifold of electronic states. II. Application to the many-body Anderson-Holstein model. *J. Chem. Phys.* **2015**, *142*, 084110.
(53) Dou, W.; Nitzan, A.; Subotnik, J. E. Surface hopping with a manifold of electronic states, III: transients, broadening and the Marcus picture. *J. Chem. Phys.* **2015**, *142*, 234106.
(54) Schmidt, J. R.; Parandekar, P. V.; Tully, J. C. Mixed quantum-classical equilibrium: Surface hopping. *J. Chem. Phys.* **2008**, *129*, 044104.
(55) Parandekar, P. V.; Tully, J. C. Mixed quantum-classical equilibrium. *J. Chem. Phys.* **2005**, *122*, 094102.
(56) Dou, W.; Nitzan, A.; Subotnik, J. E. Frictional effects near a metal surface. *J. Chem. Phys.* **2015**, *143*, 054103.
(57) Head-Gordon, M.; Tully, J. C. Molecular dynamics with electronic frictions. *J. Chem. Phys.* **1995**, *103*, 10137.
(58) Bode, N.; Kusminskiy, S. V.; Egger, R.; von Oppen, F. Current-induced forces in mesoscopic systems: A scattering-matrix approach. *Beilstein J. Nanotechnol.* **2012**, *3*, 144.
(59) Dou, W.; Subotnik, J. E. Electronic friction near metal surfaces: A case where molecule-metal couplings depend on nuclear coordinates. *J. Chem. Phys.* **2017**, *146*, 092304.
(60) Dou, W.; Subotnik, J. E. A broadened classical master equation approach for nonadiabatic dynamics at metal surfaces: Beyond the weak molecule-metal coupling limit. *J. Chem. Phys.* **2016**, *144*, 024116.
(61) Dou, W.; Subotnik, J. E. A many-body states picture of electronic friction: The case of multiple orbitals and multiple electronic states. *J. Chem. Phys.* **2016**, *145*, 054102.
(62) Note that in eq 9, we have kept only the zeroth-order gradient expansion of the term $\hat{\hat{\mathcal{L}}}_{bs}\hat{\rho}$ in eq 6. As such, one might argue that eq 9 is not balanced: after all, in eq 9, we have included all first-order gradient corrections to the other term in eq 6, $\left(-\frac{i}{\hbar}[\hat{H}_s, \hat{\rho}]\right)$. To justify this apparent contradiction, let us consider an alternative route to the QCLE-CME (eq 9). Namely, consider the Liouville equation for the total density matrix (system nuclei plus system electrons plus electronic bath), $\partial_t\hat{\rho}_{tot} = -i/\hbar[\hat{H}, \hat{\rho}_{tot}]$. If we now take the Wigner transform, we find:

$$\begin{aligned}\partial_t\hat{\rho}_{tot}^{el} &= \frac{1}{2}\{\hat{H}_{el}, \hat{\rho}_{tot}^{el}\} - \frac{1}{2}\{\hat{\rho}_{tot}^{el}, \hat{H}_{el}\} - i/\hbar[\hat{H}_{el}, \hat{\rho}_{tot}^{el}] \\ &= \frac{1}{2}\{\hat{H}_s^{el}, \hat{\rho}_{tot}^{el}\} - \frac{1}{2}\{\hat{\rho}_{tot}^{el}, \hat{H}_s^{el}\} - i/\hbar[\hat{H}_s^{el}, \hat{\rho}_{tot}^{el}] \\ &\quad - i/\hbar[\hat{H}_c, \hat{\rho}_{tot}^{el}] - i/\hbar[\hat{H}_b, \hat{\rho}_{tot}^{el}]\end{aligned}$$

Here, we have invoked the Condon approximation, that is, the fact that $\hat{H}_c$ does not depend on position in eq 4. At this point, we apply perturbation theory and trace over the bath, defining $\hat{\rho}_{el} \equiv tr_b(\hat{\rho}_{tot}^{el})$. Doing so, we find that the latter term $(i/\hbar[\hat{H}_c, \hat{\rho}_{tot}^{el}])$ yields the term $\hat{\hat{\mathcal{L}}}_{bs}^{el}(\mathbf{R})\hat{\rho}_{el}(t)$ in eq 9. Thus, the original zeroth order gradient expansion can be justified by assuming the Condon approximation and taking the limit of slow classical nuclei and fast electrons, such that electronic relaxation occurs at one instantaneous nuclear configuration.
(63) Sifain, A. E.; Wang, L.; Prezhdo, O. V. Mixed quantum-classical equilibrium in global flux surface hopping. *J. Chem. Phys.* **2015**, *142*, 224102.
(64) Nitzan, A. *Chemical Dynamics in Condensed Phases: Relaxation, Transfer and Reactions in Condensed Molecular Systems*; Oxford University Press, 2006.
(65) Lindblad, G. On the generators of quantum dynamical semigroups. *Commun. Math. Phys.* **1976**, *48*, 119−130.
(66) Jain, A.; Alguire, E.; Subotnik, J. E. An Efficient Augmented Surface Hopping Algorithm That Includes Decoherence for Use in Large-Scale Simulations. *J. Chem. Theory Comput.* **2016**, *12*, 5256.
(67) Landry, B. R.; Falk, M. J.; Subotnik, J. E. Communication: The correct interpretation of surface hopping trajectories: How to calculate electronic properties. *J. Chem. Phys.* **2013**, *139*, 211101.

DOI: 10.1021/acs.jctc.7b00094
J. Chem. Theory Comput. 2017, 13, 2430−2439